Mechanism of Above-Threshold Dissociation of Hydrogen and Deuterium Molecular Ions#

Michihiko SUGAWARA, Miwa KATO,† and Yuichi FUJIMURA*
Department of Chemistry, Faculty of Science, Tohoku University, Sendai 980
† Hitachi Research Laboratory, Hitachi 319-12

(Received May 13, 1993)

The mechanism of above-threshold dissociation (ATD) of both hydrogen and deuterium molecular ions has theoretically been investigated. A quantum-mechanical, time-dependent nuclear wave-packet theory has been applied to evaluation of the kinetic energy distributions of H_2^+ and D_2^+ photodissociations. The time-dependent shift of the kinetic energy distribution to the low energy side, which is common to both H_2^+ and D_2^+ ATD, is interpreted in terms of dynamic Stark shift. The different behavior in the intensity ratio of the kinetic energy distribution between H_2^+ and D_2^+ ATD is qualitatively explained by applying the Landau–Zener model to radiative coupling between the ATD channels involved.

Molecules in strong laser fields bring about interesting phenomena which can not be interpreted in ordinary perturbation theory.[1—5] Here, "strong" means that the magnitude of the dynamic Stark shift is the same order as the vibrational frequency of the molecule of interest. Above-threshold dissociation (ATD) of molecules is one of such phenomena.[6,7] This consists of photodissociation processes above the dissociation threshold after bound–free and free–free transitions. In a previous paper,[8] referred to as **I** hereafter, we have presented a quantum mechanical, time-dependent nuclear wave packet theory of ATD of hydrogen molecular ions under femtosecond strong laser-field conditions. The investigation of the ATD processes gives us fundamentals in understanding the mechanisms of dissociations of polyatomic molecules in strong laser fields.[9]

In Fig. 1 are shown several channels for the photodissociations of hydrogen molecular ions irradiated by laser with photon energy $\hbar\omega = 30300\ \mathrm{cm}^{-1}$. Two potential curves of $1s\sigma_g$ and $2p\sigma_u$ are associated with the photodissociation processes. Channel 1 is the one-photon dissociation channel. Channel 2 and 4 are related to the ATD in the ground electronic state, Channel 5 to the ATD in the excited state. These ATD processes can be neglected in the weak laser field. Channel 3 which is the resonant three-photon dissociation is the ATD in the excited state. This channel is the main photodissociation channel in the weak laser field. As the laser intensity increases the yield of the photodissociation from Channel 3 decreases, but on the other hand, that from Channel 2 increases. This can be qualitatively understood based on the Franck–Condon principle for optical transitions. As the laser intensity increases, stimulated emission takes place at near $R = 3.7a_0$ rather than further photon absorption. At this molecular configuration, the kinetic energy in state $2p\sigma_u$ is equal to that in $1s\sigma_g$. The channel coupling induced by radiative interaction brings about the change in the kinetic energy distribution between Channels 2 and 3. Stimulated emission takes place as the radiative coupling. In **I**, the important contribution of the stimulated emission has been discussed from the point of view of the nuclear wave packet propagation. Quite recently, Abou-Rachid et al. have studied the mechanism for the formation of fragment kinetic energy spectra of H_2^+ in ultra short pulses.[10] The variations in the kinetic energy distribution reflect the interplay between local induced transitions and accelerating and decelerating action of the field-free repulsive and attractive potentials.[10]

The purpose of this paper is to investigate ATD mechanism, and confirm the important role of the radiative interaction between Channels 2 and 3. For this purpose, we consider the photodissociation of deuterium molecular ions as well as that of hydrogen molecular ions under strong nonstationary laser field conditions. We evaluate the kinetic energy distribution of the photodissociation fragments by using the time-dependent nuclear wave packet theory. The intensity of the kinetic energy distribution of Channel 2 is stronger than that of Channel 3 in the photodissociation of D_2^+ compared with the case of H_2^+. This is qualitatively explained in terms of the Landau–Zener model for the dressed potential crossing near $R = 3.7a_0$. Time-dependent kinetic energy shifts to the low energy side are due to the dynamic Stark effect taking place during the irradiation of the nonstationary laser. The model calculation shows a sub-structure in the kinetic energy distribution of the fragments of both H_2^+ and D_2^+ photodissociations. The structure formation is discussed on the basis of the creation of the coherent wave packets during the ATD processes.

In the next section, a theoretical treatment of the time-dependent wave packet propagation in the strong nonstationary laser field is described. In the final section, similar and different behaviors in the kinetic energy distributions of H_2^+ and D_2^+ fragments are discussed on the basis of the time-dependent dynamic Stark shift and Landau–Zener model.

Theoretical

To treat the molecule-radiation interaction quantum

#This paper is dedicated to the late Professor Hiroshi Kato.

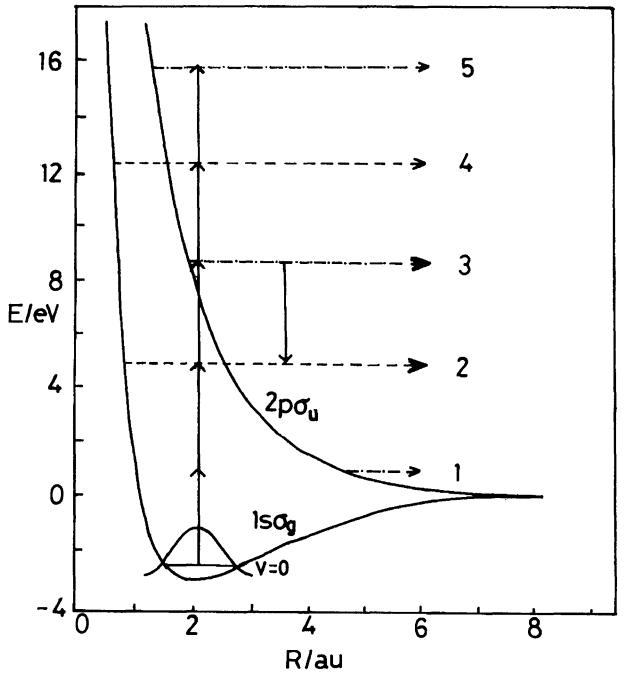

Fig. 1. Possible photodissociation channels of hydrogen molecular ions excited by photon with wavelength $\lambda=329.7$ nm. $1s\sigma_g$ and $2p\sigma_u$ refer to the ground and excited states, respectively. Channel 1 denotes the one-photon dissociation from $2p\sigma_u$ state. Channels 2 and 4 are two- and four-photon ATD processes from $1s\sigma_g$ state, respectively. Channels 3 and 5 denote three- and five-photon ATD processes, respectively. The down arrow represents a free–free transition induced by radiative coupling (stimulated emission). This transition takes place at $R\cong 3.7a_0$ on the basis of the Franck–Condon principle.

mechanically, we adopt the dressed basis set. The total system Hamiltonian is expressed as the summation of the Hamiltonian of molecular ion $\hat{\boldsymbol{H}}_{\mathrm{M}}$, the radiation field $\hat{\boldsymbol{H}}_{\mathrm{R}}$, and the time-dependent molecule-radiation interaction $\hat{\boldsymbol{H}}_{\mathrm{MR}}(t)$ as

$$\hat{\boldsymbol{H}}(t) = \hat{\boldsymbol{H}}_{\mathrm{M}} + \hat{\boldsymbol{H}}_{\mathrm{R}} + \hat{\boldsymbol{H}}_{\mathrm{MR}}(t). \tag{1}$$

We consider the wave-packet dynamics on two electronic states of molecular ions, which are the ground state $1s\sigma_g$ denoted by $|g\rangle$, and the excited state $2p\sigma_u$ denoted by $|e\rangle$. Within the adiabatic approximation the molecular ion Hamiltonian $\hat{\boldsymbol{H}}_{\mathrm{M}}$ is given as

$$\hat{\boldsymbol{H}}_{\mathrm{M}} = |g\rangle\left[\hat{K} + V_g(\hat{R})\right]\langle g| + |e\rangle\left[\hat{K} + V_e(\hat{R})\right]\langle e|, \tag{2}$$

where $\hat{K}$ and $\hat{R}$ denote the kinetic energy operator and the position operator of the nuclear motion, respectively, and $V_g(\hat{R})$ and $V_e(\hat{R})$ denote the adiabatic potentials on the electronic ground and excited states. Adiabatic potentials $V_g(\hat{R})$ and $V_e(\hat{R})$ are taken to be[11]

$$V_\alpha(\hat{R}) = D_0\left\{\exp\left[-2\beta\left(\hat{R}-R_e\right)\right] - 2t_\alpha\exp\left[-\beta\left(\hat{R}-R_e\right)\right]\right\}, \tag{3}$$

where $D_0=22522.852\ \mathrm{cm}^{-1}$, $\alpha=\{g,e\}$, $\beta=0.72$, $R_e=2.0a_0$, $t_g=1.0$, and $t_e=-1.11$. The radiation field Hamiltonian is expressed as

$$\hat{\boldsymbol{H}}_{\mathrm{R}} = \hbar\omega a^\dagger a, \tag{4}$$

here ω denotes the frequency of the radiation field, and a and $a^\dagger$ denote the annihilation and creation operators of photon, respectively. The interaction Hamiltonian between the molecular ion and radiation field $\hat{\boldsymbol{H}}_{\mathrm{MR}}(t)$ is given as

$$\hat{\boldsymbol{H}}_{\mathrm{MR}}(t) = -iA(t)f_{eg}(\hat{R})\left(a+a^\dagger\right)\left(|e\rangle\langle g| - |g\rangle\langle e|\right), \tag{5}$$

where $A(t)$ is the envelope function introduced to express the time-dependence of the radiation field. In Eq. 5, $f_{eg}(\hat{R})$ is defined as

$$f_{eg}(\hat{R}) = \frac{V_e(\hat{R}) - V_g(\hat{R})}{\sqrt{2\hbar\varepsilon_0\omega L^3}}\varepsilon\cdot\hat{\mu}_{eg}(\hat{R}), \tag{6}$$

where ε denotes the polarization unit-vector of the radiation field, L^3 the box quantization volume, and ε_0 the electric permittivity of free space, and $\hat{\mu}_{eg}(\hat{R})$ the transition dipole moment vector. The matrix element of the transition dipole moment is assumed to be expressed as[11]

$$\mu_{ge}(\hat{R}) = \mu + \frac{\mu'}{\beta y}\left\{1 - \exp\left[-\beta y\left(R-R_e\right)\right]\right\}, \tag{7}$$

where $\mu=1.07a_0\cdot e$, $\mu'=0.396e$, and $y=-0.055$, where e denotes the elementary electric charge.

The time-dependent Schrödinger equation is given as

$$\frac{\mathrm{d}}{\mathrm{d}t}|\Psi(t)\rangle = -\frac{i}{\hbar}\hat{\boldsymbol{H}}(t)|\Psi(t)\rangle, \tag{8}$$

where $|\Psi(t)\rangle$ is the state vector of the total system. To reform Eq. 8 into matrix representation, we introduce the basis set expressed as[12]

$$\begin{aligned}&\{|0\rangle,|1\rangle,\cdots,|m\rangle,\cdots|n-1\rangle,|n\rangle\}\\ &\equiv\{|R_i\rangle\otimes|g\rangle\otimes|N\rangle,|R_i\rangle\otimes|e\rangle\otimes|N-1\rangle,\\ &\qquad\vdots\\ &\quad|R_i\rangle\otimes|g\rangle\otimes|N-n+1\rangle,|R_i\rangle\otimes|e\rangle\otimes|N-n\rangle\},\end{aligned} \tag{9}$$

where $|N\rangle$ denotes the number state of the radiation field, and $\{|R_i\rangle\}$ denotes the discretized basis set of the position coordinate of the nuclear motion. It should be noticed that the dressed state basis set $\{|m\rangle\}$ is expressed in terms of the tensor product of molecular electronic states and radiation number states, and the number m refers to the number of absorbed photons.

The nuclear wave packets on the lth basis state $|l\rangle$, $\phi_l(t)$, is defined as

$$\phi_l(t) = \phi_l(R_i, t) = \langle l|\Psi(t)\rangle \quad (l = 0, 1, \cdots, n). \tag{10}$$

Using the dressed basis set in Eq. 9 and the definition of the wave packets corresponding to each photon absorption given in Eq. 10, the time-dependent Schrödinger equation is given in matrix form as

$$\begin{aligned}
&\frac{\mathrm{d}}{\mathrm{dt}}\begin{pmatrix}\phi_1(t)\\ \phi_2(t)\\ \vdots\\ \phi_n(t)\end{pmatrix}\\
&= -\frac{i}{\hbar}\begin{pmatrix} H_{11} & H_{12}(t) & \cdots & H_{1n}(t)\\ H_{21}(t) & H_{22} & \cdots & H_{2n}(t)\\ \vdots & \vdots & \ddots & \vdots\\ H_{n1}(t) & H_{n2}(t) & \cdots & H_{nn}\end{pmatrix}\begin{pmatrix}\phi_1(t)\\ \phi_2(t)\\ \vdots\\ \phi_n(t)\end{pmatrix}.\\
&\equiv -\frac{i}{\hbar}\boldsymbol{H}(t)\phi(t)
\end{aligned} \tag{11}$$

The diagonal matrix elements of $\boldsymbol{H}(t)$ is expressed as

$$H_{ll}(R_i, R_j) = \frac{k_u\hbar^2}{2m\Delta R} + V_l(R_i)\,\delta_{ij} + N\hbar\omega\delta_{ij}, \tag{12}$$

with

$$\begin{aligned}
&k_0 = \frac{73766}{25200},\ k_1 = -\frac{42000}{25200},\ k_2 = \frac{6000}{25200},\\
&k_3 = -\frac{1000}{25200},\ k_4 = \frac{125}{25200},\ k_5 = -\frac{8}{25200},
\end{aligned} \tag{13}$$

where $i \pm u = j (u = 0, 1, \cdots, 5)$, $l = \{g, e\}$, and ΔR denotes the size of the spatial grid. In the practical calculation performed in this study, ΔR is taken to be 0.00567 au. The first term of Eq. 12 originates from the kinetic energy term of the molecular Hamiltonian $\hat{\boldsymbol{H}}_{\mathrm{M}}$. The off diagonal matrix element is given as

$$H_{ll'}(R_i, R_j) = -iA(t) f_{eg}(R_i)\,\delta_{ij}. \tag{14}$$

In this work, we utilize a sliced propagator method to get the time evolution of wave packets.[13] The formal solution of Eq. 11 is given as

$$\phi(t) = \hat{T}\exp\left[-\frac{i}{\hbar}\int_{t'=0}^{t'=t}\mathrm{d}t'\boldsymbol{H}(t')\right]\phi(0) \equiv U(t)\phi(0), \tag{15}$$

where $\hat{T}$ denotes the time ordering operator, and $U(t)$ is the time evolution operator. By introducing the infinitesimal time step Δt, and the iteration of the operation of sliced propagator $U(\Delta t)$ defined as

$$\phi(t + \Delta t) = \exp\left[-\frac{i}{\hbar}\boldsymbol{H}(t)\Delta t\right]\phi(t) \equiv U(\Delta t)\phi(t), \tag{16}$$

one can obtain the time evolution of wave packets $\{\phi_l(t)\}$. We expand the sliced propagator in a power series as

$$\begin{aligned}
U(\Delta t) &= \exp\left[-\frac{i}{\hbar}\boldsymbol{H}(t)\Delta t\right]\\
&= 1 + \left(\frac{-i\boldsymbol{H}(t)\Delta t}{\hbar}\right) + \frac{1}{2!}\left(\frac{-i\boldsymbol{H}(t)\Delta t}{\hbar}\right)^2\\
&\quad + \frac{1}{3!}\left(\frac{-i\boldsymbol{H}(t)\Delta t}{\hbar}\right)^3 + \cdots
\end{aligned} \tag{17}$$

The time step Δt is taken to be small so that it satisfies the condition $|H(t)\Delta t| \leq 0.4\hbar$ at any time.

The time evolution of nuclear wave packets in momentum space $\varphi_l(k,t)$ can be obtained by applying Fourier transform to the wave packets in coordinate representation as $\varphi_l(k, t) = \mathscr{F}[\phi_l(R, t)]$, where $\mathscr{F}$ denotes Fourier transform that is performed as FFT (Fast Fourier transform) in the numerical calculation. To compare the ATD dynamics of H_2^+ and D_2^+ from the point of view of the kinetic energy distribution of the dissociation fragments, we define the kinetic energy distribution $\rho_l(K,t)$, with the simple relation between momentum k and kinetic energy K, $k = \sqrt{2mK}/\hbar$, as

$$\rho_l(K, t) = \left|\varphi_l\left(\sqrt{2mK}/\hbar, t\right)\right|^2 + \left|\varphi_l\left(-\sqrt{2mK}/\hbar, t\right)\right|^2. \tag{18}$$

In the present calculation, dressed state basis is introduced with $n=7$, in which up to 7 photon absorption processes are taken into account. The photon number N in Eq. 9 is determined from the intensity of radiation field I (TW cm^{-2}) by using the relation

$$N = \frac{2\pi L^3 I}{c\hbar\omega}. \tag{19}$$

Here one photon energy of radiation field $\hbar\omega$ is taken to be 30300 cm^{-1} as used in **I**, which is above the dissociation energy D_0. Initial wave packet is taken to be the vibrational ground state of the electronic ground state as shown in Fig. 1.

Results and Discussion

To investigate the ATD mechanism, we present the model calculation of the kinetic energy distribution of both H_2^+ and D_2^+ ATD fragments as a function of the observation time. The pulse shape $A(t)$ of the nonstationary laser was assumed to take the form,

$$\begin{aligned}
A(t) &= A_0 \exp\left[-2(t - t_0)^2/{\sigma_p}^2\right] \quad \text{for } t \leq t_0\\
&= A_0 \qquad\qquad\qquad\qquad\quad \text{for } t > t_0.
\end{aligned} \tag{20}$$

Here parameter σ_p is chosen for the pulse intensity to become a maximum in 90 fs (t_0=90 fs) with a half maximum at 30 fs.

Figure 2 shows the kinetic energy distributions of H_2^+ dissociation observed at time t=80, 100, and 140 fs. The intensity of the laser used is $I = 5.6\times10^{14}$ W cm^{-2}.

The kinetic energy distribution consists of two main energy structures. The structure at the low energy side originates from the ATD through Channel 2, and that at the high energy side originates from the ATD through Channel 3. We can see that each structure has a sub-structure.

Figure 3 shows the kinetic energy distribution of D_2^+ dissociation at $t=100$, 120, and 140 fs. The same intensity of the pulsed laser as that in Fig. 2 is used in calculating the distribution. The common characteristic behavior of the kinetic energy distributions in Figs. 2 and 3 is that first the center of gravity of the each structure shift to the low kinetic energy side, and, secondly the manifold of the sub-structure increases in number as the observation time develops. There is no detectable shift in both H_2^+ and D_2^+ ATD processes for longer time than $t=140$ fs. This suggests that the kinetic energy distribution at 140 fs is actually close to the final dissociated one. The shifts of the center of gravity in Figs. 2 and 3 are due to the potential energy changes

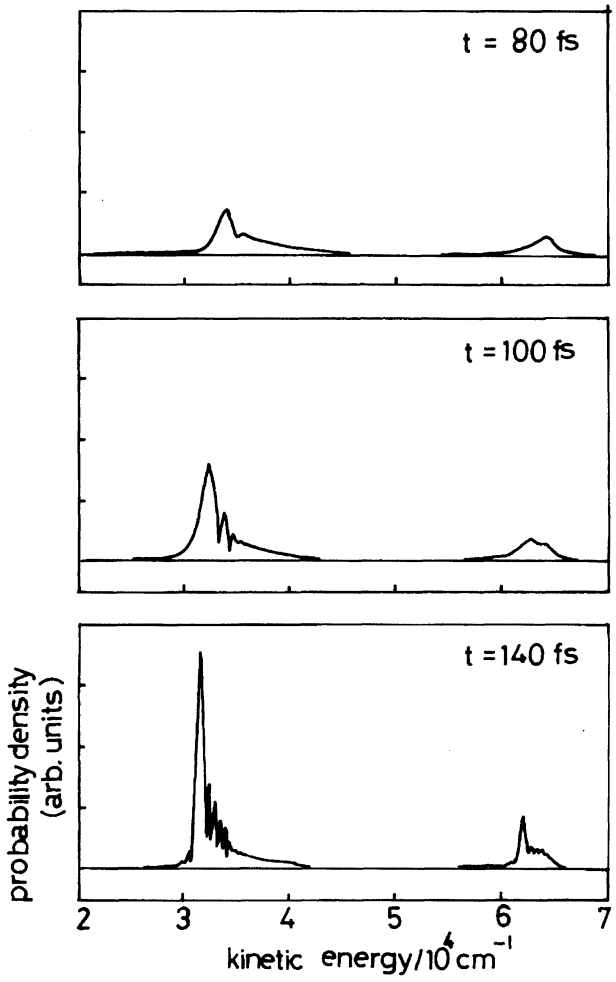

Fig. 2. Kinetic energy distributions of hydrogen molecular ions at 80, 100, and 140 fs. Nonstationary laser characterized by Eq. 20 with peak intensity 5.6×10^{14} W cm^{-2} was assumed.

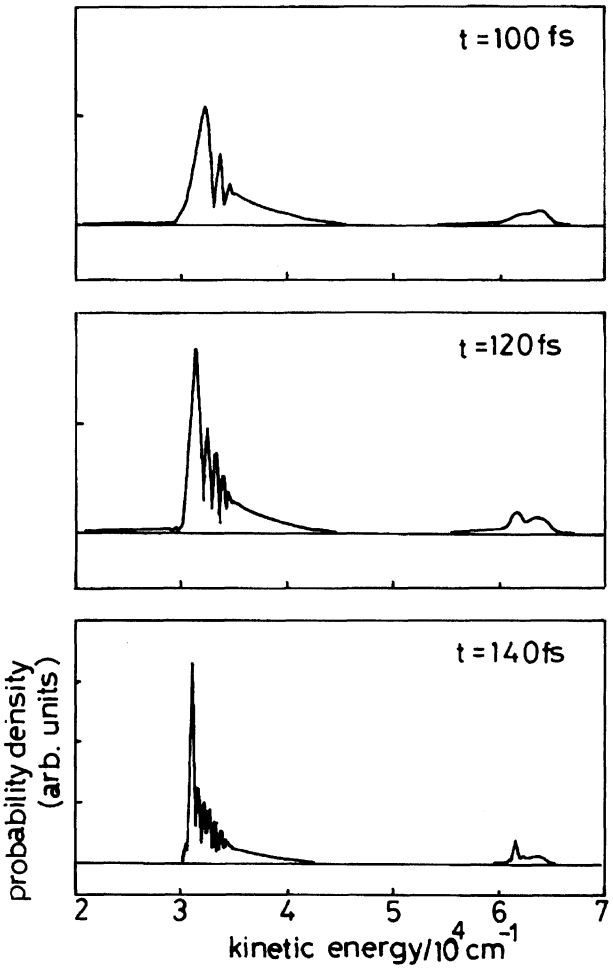

Fig. 3. Kinetic energy distributions of deuterium molecular ions at 100, 120, and 140 fs. The same nonstationary laser as that in Fig. 2 was assumed.

between $1s\sigma_g$ and $2p\sigma_u$ states under strong laser fields. This shift is so-called dynamic Stark shift.[14] The term "dynamic Stark shift" is usually used under stationary radiation field conditions, that is, the shift is taken as a function of the laser intensity. It should be noted that the time-dependent shifts in Figs. 2 and 3 reflect the potential energy change in the nonstationary laser field used.

Let us discuss the sub-structure formation. There are possibilities of the sub-structure formation independent of the radiative coupling between Channels 2 and 3. One of the main possibilities is due to the creation of the dressed vibrational states in the excitation process. To see the possibility of such a structure formation, we have performed a calculation of the time-dependent kinetic energy distribution of the fragments produced by the direct photodissociation excited by one photon energy $3\hbar\omega$. We have obtained a structureless, broad kinetic energy distribution totally different from that excited by photon energy $\hbar\omega$. This means that the sub-structure formation is not due to the creation of the

dressed vibrational states in the excitation process, but to interactions between Channels 2 and 3. The most possible origin of the sub-structure formation is due to the interference between the coherent wave packets produced by the radiative coupling. For example, consider the wave packet associated with Channel 2. This wave packet is expressed by the sum of the wave packet created by just two-photon absorption and those produced by the radiative coupling through Channel 3. The resultant kinetic energy distribution consists of the direct contribution from each wave packet and of the interference between the wave packets. The constructive and destructive interferences bring about the sub-structure in the kinetic energy distribution of the ATD fragments.

It should be noted in Figs. 2 and 3 that the intensity ratio of kinetic energy distribution of Channel 3 to Channel 2 in the D_2^+ ATD processes is larger than that in the H_2^+ ATD process. This difference in the intensity ratio between D_2^+ and H_2^+ ATD processes can be qualitatively explained by applying the Landau–Zener model to the radiative coupling between Channels 2 and 3.[15—17] The transition probability from Channel 3 to Channel 2, $P_{3\to 2}$ is given by

$$P_{3\to 2} = 1 - P, \tag{21}$$

where P represents the transition probability between the radiatively coupled states. This probability is expressed in the Landau–Zener model as

$$P = \exp\left[-2\gamma\right], \tag{22}$$

where $\gamma = \frac{\pi|V_{32}|^2}{\hbar\nu(\mathrm{d}\Delta E/\mathrm{d}R)}$, in which ν is the velocity at the dressed potential crossing point, V_{32} denotes the magnitude of the radiative coupling matrix element between Channel 3 and Channel 2, and $\frac{\mathrm{d}\Delta E}{\mathrm{d}R}$ the difference in the force between $1s\sigma_g$ and $2p\sigma_u$ states at the crossing point. The velocity of the relative motion of H_2^+, ν_H and that of D_2^+, ν_D at the crossing point satisfy the relation $\nu_H = \sqrt{2}\nu_D$. This results in $P_D < P_H$ where P_D and P_H are the transition probability between the radiatively coupled states of D_2^+ and that of H_2^+, respectively. That is the magnitude of the radiative transition probability from Channel 3 to Channel 2 in D_2^+ photodissociation is larger than that in H_2^+ photodissociation as shown in Figs. 2 and 3. In other words, the adiabaticity in the D_2^+ ATD process increases compared with that in H_2^+.

Figure 4 schematically shows the difference in the ATD probability between D_2^+ and H_2^+ photodissociations. The curves denoted by $|3\rangle$ and $|2\rangle$ represent the dressed potentials of Channels 3 and 2 with photons $N-3$ and $N-2$, respectively. The ability of the transition induced by the radiative coupling is represented by the magnitude of the arrow indicated in Fig. 4.

In summary, in this paper we have presented a theoretical treatment of the ATD mechanism of both hydrogen and deuterium molecular ions excited by a nonstationary, strong laser. The radiative interaction between two-photon and three-photon absorbed states makes an important contribution to the ATD mechanism. This has been clarified from the different behavior in the intensity ratio of the kinetic energy distribution between H_2^+ and D_2^+ ATD, which can be qualitatively explained by using the Landau–Zener model.

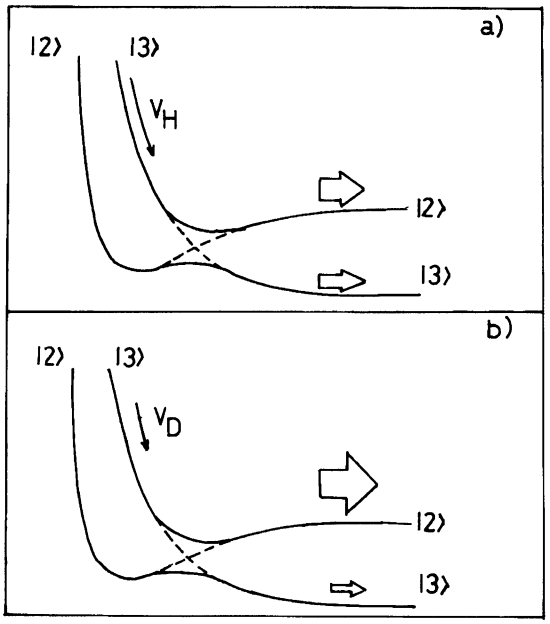

Fig. 4. Dressed state representation of the radiative coupling between Channels 2 and 3. a) and b) show the H_2^+ and D_2^+ photodissociations, respectively. The broken lines refer to the zeroth order dressed potentials. The full lines represent the dressed potentials taken into account the radiative coupling. ν_H and ν_D refer to the velocity of hydrogen molecular ion fragment and that of deuterium one, respectively. The arrows represent the magnitudes of the transition probability from Channel 3 to Channel 2, and those of the existing probability at the initial channel.

The present research is supported in part by Grant-in-Aid for Scientific Research on Priority Area "Theory of Chemical Reactions" from the Ministry of Education, Science and Culture.

References

1) A. D. Bandrauk, "Atomic and Molecular Processes with Short Intense Laser Pulses," Plenum Press, New York (1988).

2) H. Rottke, B. Wolff, M. Brickwedde, D. Feldmann, and K. H. Welge, in "Proceedings of the 5th International Conference on Multiphoton Processes," ed by G. Mainfray and P. Agostini, Paris (1990), p. 33.

3) T. F. George, I. H. Zimmerman, J. M. Yuan, J. R. Laing, and P. L. de Vries, *Acc. Chem. Res.*, **10**, 449 (1977).

4) Y. Ohtsuki, Y. Fujimura, and S. H. Lin, *J. Chem.*

Phys., **93**, 3012 (1990).
5) D. J. Tannor and S. A. Rice, *Adv. Chem. Phys.*, **70**, 441 (1990).
6) X. He, O. Atabek, and A. Giusti-Suzur, *Phys. Rev., Sect. A*, **A38**, 5586 (1988).
7) A. Giusti-Suzur, X. He, O. Atabek, and F. H. Mies, *Phys. Rev. Lett.*, **64**, 515 (1990).
8) M. Sugawara, M. Kato, and Y. Fujimura, *Chem. Phys. Lett.*, **184**, 203 (1991).
9) S. H. Lin, Y. Fujimura, H. J. Neusser, and E. W. Schlag, "Multiphoton Spectroscopy of Molecules," Academic Press, New York (1984), Chap. 7, p. 197—207.
10) H. Abou-Rachid, T. Tung Nguyen-Dang, R. K. Chaudhury, and X. He, *J. Chem. Phys.*, **97**, 5497 (1992).
11) F. V. Bunkin and I. I. Tugov, *Phys. Rev. Sect. A*, **A8**, 601 (1973).
12) M. Sugawara and Y. Fujimura, *Chem. Phys.*, in press.
13) H. Tal-Ezer and R. Kosloff, *J. Chem. Phys.*, **81**, 3967 (1984).
14) P. L. Knight and P. W. Milonni, *Phys. Rep.*, **66**, 21 (1980).
15) L. D. Landau and E. M. Lifshitz, "Quantum Mechanics, Non-relativistic Theory," 2nd ed, Addison-Wesley, New York (1965), p. 322.
16) A. M. F. Lau and C. K. Rhodes, *Phys. Rev. Sect. A*, **A15**, 1570 (1977).
17) T. Sizer, II and M. G. Raymer, *Phys. Rev. Sect. A*, **A36**, 2643 (1987).